

STRUCTURAL GEOLOGY

Mancktelow, Neil S.

Department of Earth Sciences, Swiss Federal Institute of Technology, CH–8092 Zürich, Switzerland

Keywords: Deformation, strain, stress, folds, faults, modeling

Contents

1. Introduction
 2. Stress and Strain
 - 2.1. Stress
 - 2.2. Measurement of Stress
 - 2.3. Strain
 - 2.4. Measurement of Strain
 3. Geometry
 - 3.1 Common Deformation Structures
 - 3.2 Influence of Initial Irregularities
 - 3.3 Polyphase Deformation
 4. Kinematics
 5. Dynamics
 6. Tectonic Modeling
 - 6.1 Analytical Models
 - 6.2 Numerical Models
 - 6.3 Physical Models
 7. Outlook
- Glossary
Bibliography
Biographical Sketch

Summary

Structural geology attempts to unravel the deformation history that led to the often quite complicated structures now observed in mountain belts. Field mapping and laboratory observation may establish the current geometry and give constraints on the kinematics, i.e., the direction and sense of movement, of major displacement zones. Under favorable circumstances, the finite strain can also be quantified (using strain markers such as fossils, oolites, reduction spots, conglomerates, etc.), though usually only in scattered locations. Geometric overprinting criteria may allow a consistent history of deformation phases to be established, related to structures with a particular orientation, style and possibly kinematics. As natural observations represent only a single time slice in the history of these structures, understanding the progressive development of deformation structures requires some form of modeling to scale the long geological times involved (commonly on the order of millions or tens of millions of years). This involves either analytical approximation based on continuum or fracture mechanics, physical scale modeling, or increasingly in recent times, numerical modeling. The necessary inputs for all these models are the rheology of the rock materials (though in an inverse fashion, the

predicted natural geometry can help constrain the possible rheology), the boundary conditions, and the initial configuration. Since it is the original irregularities that grow exponentially, as the result of mechanical instability under load, to form the final observed structures, the distribution and geometry of these initial, often small features should not be overlooked as they can have an important influence on the final shape. Although modeling is critical to understanding deformation processes, field studies still provide the ultimate natural control on potential mechanisms and careful field observation remains the fundamental basis of structural geology.

1. Introduction

Structural geology is the study of deformed rocks. It covers both direct field observation and mapping of the geometry of structures developed due to deformation (folds, faults, rock cleavage, shape and crystallographic preferred orientation etc.) and modeling or experimentation to establish the mechanical response of rocks to deformation. For small loads, short time periods and/or low temperature, rocks behave elastically and deformation is recoverable on removal of the load. If the load is progressively increased, the rock will at some stage fracture, with the necessary load for fracture increasing approximately linearly with confining pressure. Below this fracture limit, rocks will flow over long time periods, the tendency to flow being strongly promoted by increased temperature. Since both pressure and temperature increase with depth below the surface, there is a transition from dominantly elastic-brittle (fracture) behavior to dominantly elastoviscous behavior at some depth (commonly at approximately 10-15 km depth, depending on the rock type, thermal structure, rate of loading etc.). This range in behavior is not specific to rocks and much of our understanding of rock rheology and associated deformation mechanisms derives from metallurgy and material science. However, what is different in geosciences is the enormous range of length and time scales involved. Observational scales range from ca. 10^{-7} m (e.g., crystal scale deformation examined under the electron microscope) to 10^3 m (the scale of individual mountain belts) and geological time scales range from the order of seconds for earthquakes up to 10's to 1000's of millions of years (10^{14} - 10^{15} s).

The earth is a dynamic planet, on which an outer skin of colder stiff plates (the lithosphere) moves across a weak viscous substrate (the asthenosphere) weakened by the presence of partially molten rock (see *Plate Tectonics of Continents and Oceans*). As end-member geometries, plates can either diverge, with the space being filled by newly crystallized material derived from the partially molten asthenosphere (constructive plate margin), or converge, with one plate descending below the other (destructive plate margin or subduction zone), or glide past each other with the velocity vectors parallel to the boundary (conservative margin). Most plate margins lie somewhere between these extreme end-members. Rates of relative plate motion are on the order of centimeters per year. As discussed in detail below, deformation or strain reflects gradients in displacement and the highest strain rates consequently occur at plate margins, though weaker intraplate deformation may be locally important (e.g., low amplitude, large wavelength buckling of the plate in the Indian ocean). Lower density continental crustal material riding on these moving plates can become directly involved in this deformation. In broad terms, the two most important examples are (1) development of a new divergent margin, leading to stretching and thinning of the crust

and (2) collision between two continents across a convergent margin. The major mountain belts, such as the Alps and the Himalayas, are classic examples of collision of continental blocks and are characterized by a wide range of deformation structures — these are textbook regions for structural geology.

2. Stress and Strain

Deformation or strain is the direct result of the forces applied: these may be body forces (e.g., gravitational force), which act on a volume, or surface forces (e.g., the forces applied to the edge of a plate). Surface forces are measured as the stress, or force per unit area. Strain is measured as relative changes in the length of lines (stretches) and as changes in angle (shear strain).

2.1. Stress

Stress is an instantaneous quantity that can only be determined for a specific time and in general will vary in both space and time during deformation. It is defined as the force per unit area and stress can be resolved into components acting either normal (“normal stress”) or parallel (“shear stress”) to the surface in question. If we consider a point on a small surface element ΔS with vector normal \mathbf{n} , then the surface forces ΔF_i acting on ΔS are equivalent to a single force acting at the point itself and a couple or moment tending to cause rotation around the point. The Cauchy stress principle asserts that the ratio $\Delta F_i / \Delta S$ tends to a definite limit and that the couple vanishes as ΔS approaches zero. The resulting vector dF_i / dS is called the *stress vector* (or *traction vector*) $\mathbf{t}^{(n)}$. The notation $\mathbf{t}^{(n)}$ is used to emphasize that the stress vector at a point in the continuum depends explicitly on the orientation of the particular surface element ΔS , as represented by the unit normal \mathbf{n} .

The state of stress at a point can be defined by considering the stress defined on the surfaces of a cube containing the point of interest and with edges parallel to the coordinate axes x_i , as the volume of that cube becomes infinitesimally small. For each surface, the normal stress components are written as σ_{ii} (e.g., σ_{11}) and shear components as σ_{ij} , $i \neq j$ (e.g., σ_{12}), with the orientation of the surface normal given first. At the limit as the volume decreases to zero, the values of normal and shear stress components on opposing surfaces of the cube must be equal and the state of stress can be represented by a second order tensor (equivalent to an $n \times n$ matrix of stress components σ_{ij} for $i = 1..n$, $j = 1..n$, where n is the number of dimensions). Stress equilibrium requires that there are no unbalanced rotational moments that would produce an angular acceleration, which implies that the stress tensor is also symmetric (i.e., $\sigma_{ij} = \sigma_{ji}$). Such a symmetric second order tensor has three independent components in two dimensions and six in three dimensions.

The stress vector $\mathbf{t}^{(n)}$ defined above is in general not parallel to the surface normal \mathbf{n} . However, it can readily be shown that solution of the vector equation $\mathbf{t}^{(n)} = \sigma \mathbf{n}$ (a classic eigenvalue-eigenvector problem) yields three perpendicular directions where the relationship is satisfied, the three *principal stress directions*, with corresponding *principal stress values* σ_1 , σ_2 and σ_3 . Parallelism of the stress vector and surface normal implies that only normal stresses are present on the three surfaces perpendicular to the

principal directions. This is the same as saying that the stress tensor at a point is diagonalized when transformed into a coordinate system parallel to the principal directions. It is a general property of any real symmetric tensor (or matrix) that it can be diagonalized by a suitable orthogonal transformation of the coordinate system $\mathbf{S}^P = \mathbf{O} \mathbf{S} \mathbf{O}^T$ (where orthogonality implies that the inverse of matrix \mathbf{O} is equal to its transpose \mathbf{O}^T) to give the form:

$$S_{ij}^P = \begin{bmatrix} s_1 & 0 & 0 \\ 0 & s_2 & 0 \\ 0 & 0 & s_3 \end{bmatrix}. \quad (1)$$

Compressive stress is generally assumed to be positive in structural geology (since stress at depth in the earth is invariably compressive; note that this convention is the opposite of that usually followed in engineering and continuum mechanics). From this assumption and the results above, it follows that the stress tensor at a point can be envisaged as ellipsoid, the so-called *stress ellipsoid*, with axes parallel to the principal directions, the longest axis of length σ_1 (maximum normal stress) and shortest of length σ_3 (minimum normal stress). The total stress can therefore be defined by the orientation and magnitude of the three principal stresses.

The mean stress $\sigma_m = (\sigma_{11} + \sigma_{22} + \sigma_{33}) = (\sigma_1 + \sigma_2 + \sigma_3) = (\text{trace } \sigma_{ij})/3$ is an invariant value that does not change with rotation of the coordinate system and represents the isotropic component of the stress (or the “pressure”) that tends to cause an isotropic change in shape, i.e., a volume change. The remaining anisotropic component of stress is referred to as the deviatoric stress, that is:

$$\begin{bmatrix} \sigma_{11} & \sigma_{12} & \sigma_{13} \\ \sigma_{12} & \sigma_{22} & \sigma_{23} \\ \sigma_{13} & \sigma_{23} & \sigma_{33} \end{bmatrix} = \begin{bmatrix} \sigma_{11} - \sigma_m & \sigma_{12} & \sigma_{13} \\ \sigma_{12} & \sigma_{22} - \sigma_m & \sigma_{23} \\ \sigma_{13} & \sigma_{23} & \sigma_{33} - \sigma_m \end{bmatrix} + \begin{bmatrix} \sigma_m & 0 & 0 \\ 0 & \sigma_m & 0 \\ 0 & 0 & \sigma_m \end{bmatrix}. \quad (2)$$

total stress **deviatoric stress** **mean stress**

A 2D cut through the 3D stress ellipsoid will have an elliptical shape with major and minor axes σ_1^* and σ_2^* that are not necessarily principal values. For a plane perpendicular to this section, the shear stress τ and the normal stress σ is given by:

$$\sigma = \frac{\sigma_1^* + \sigma_2^*}{2} - \frac{\sigma_1^* - \sigma_2^*}{2} \cos 2\theta \quad (3)$$

$$\tau = \frac{\sigma_1^* - \sigma_2^*}{2} \sin 2\theta \quad (4)$$

assuming compressive stress is positive and θ is the angle between the unit normal to the surface and σ_1 . These equations have the same form as the parametric representation of a circle, and are therefore often conveniently represented as the so-called Mohr circle for stress (Figure 1).

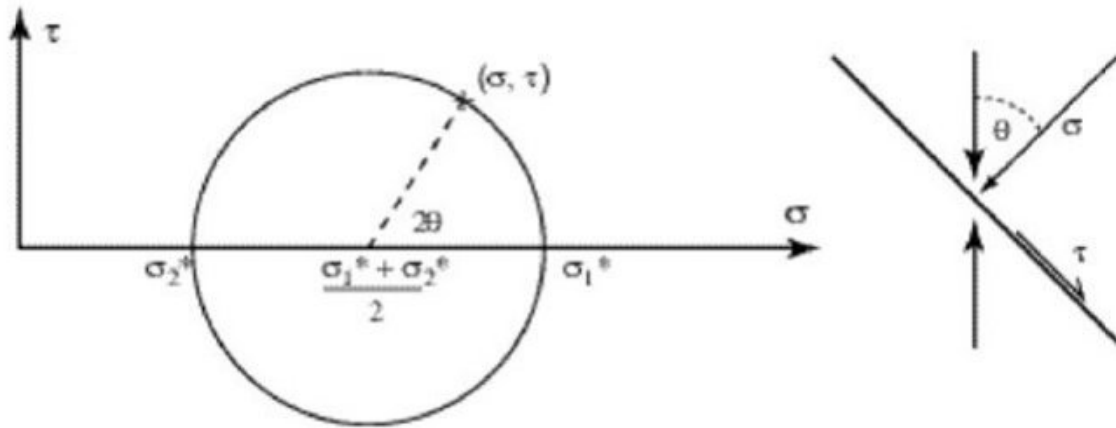


Figure 1. Mohr circle representation for stress normal and shear stress components on a plane (in two dimensions).

As the intermediate stress axis is unimportant for controlling brittle fracture and the planes of failure generally intersect in the intermediate axis, the representation for stress in the plane perpendicular to the intermediate axis (e.g., Figure 1 with $\sigma_1^* = \sigma_1$ and $\sigma_2^* = \sigma_3$) is the most commonly used.

2.2. Measurement of Stress

Stress can only be measured from the response of the material (i.e., the strain). As an instantaneous quantity, it can therefore only be determined for a particular instant in time. Stresses will have varied from place to place and with time during the development of any deformation structure that we now observe. The only way to estimate the stress history that may have been involved is by modeling the development. In practice this may be approached by approximate analytical methods or by physical or numerical modeling (Section 6). In particular, several classic studies of the distribution of elastic stresses during deformation have used photoelastic materials (e.g., gelatin), which display alternating light and dark fringes in polarized light representing contours of stress magnitude, as an analogue for rocks. In most physical models, however, it is not possible to establish the stress distribution during deformation

Fracture is a near instantaneous phenomenon and therefore could reflect the stress at the time of failure. This provides a potential approach for determining the orientation and possibly the geometry of the stress ellipsoid (and therefore the stress tensor) at some specific time in the past. If a chronology of consistently overprinting faults in a biostratigraphically dated sedimentary sequence can be established, then a stress history through time may be determined. The simplest technique involves the determination of the orientation of the three stress axes from sets of conjugate faults, with the intermediate stress axis σ_2 parallel to the intersection of the two faults, the axis of maximum compressive stress σ_1 bisecting the acute angle (usually $\sim 60^\circ$), and σ_3 bisecting the obtuse angle. Conjugate faults are not always present and most other methods assume that the movement direction on a fault plane (recognized from striae, grooves or synkinematic mineral fibers) is parallel to the direction of maximum resolved shear stress in that plane. Today, many of the methods are encoded into freely

available computer programs, though it wise to understand what the code is actually doing before the results are uncritically accepted.

The measurement of current stresses is important both for the current tectonics (neotectonics) and for practical problems of underground construction. Effective methods of measurement are discussed in detail in references given in the Bibliography.

2.3. Strain

Strain describes the change in relative position of material points that make up a body. It can be considered mathematically as a coordinate transformation $X_{ij} = a_{ij}x_j + u_i$ (standard summation notation), which can be written in matrix form as $\mathbf{X} = \mathbf{A}\mathbf{x} + \mathbf{U}$. The constant values u_i , which are independent of position, represent a rigid body translation, and are not considered further. \mathbf{A} is an $n \times n$ matrix, where n is the number of dimensions, and can be somewhat artificially (because it has little to do with the actual deformation path) split into a distortion \mathbf{D} and a rigid body rotation \mathbf{R}

$$\mathbf{A} = \mathbf{DR} \neq \mathbf{RD} . \quad (5)$$

Note that for finite strain the operation is not commutative, i.e., a finite distortion followed by a finite rotation does not produce the same result if the order of application is reversed. For example, a rigid body rotation about the x_3 axis has the form

$$\mathbf{R} = \begin{pmatrix} \cos \omega & -\sin \omega & 0 \\ \sin \omega & \cos \omega & 0 \\ 0 & 0 & 1 \end{pmatrix}, \quad (6)$$

where, by convention, ω is positive for an anticlockwise rotation. Note that the matrix is antisymmetric. The ratio of final to initial area in 2D (A/A_0), respectively volume in 3D (V/V_0), is given by the determinant of \mathbf{D} (or \mathbf{A} , since $\det \mathbf{D} = \det \mathbf{A}$, because rigid body rotation obviously does not involve volume change, i.e., $\det \mathbf{R} = 1$).

The term *plane strain* is used for deformation in which deformation takes place within a single plane, i.e., there is no change in length of lines perpendicular to this plane and the deformation can be fully described in two dimensions (i.e., by a 2×2 matrix). Two end-member plane strain geometries are defined as

$$(1) \text{ pure shear, where } \mathbf{A} = \begin{pmatrix} c & 0 \\ 0 & 1/c \end{pmatrix}, \text{ e.g., see Figure 2a, where } c = 1/2,$$

and

$$(2) \text{ simple shear, where } \mathbf{A} = \begin{pmatrix} 1 & \gamma \\ 0 & 1 \end{pmatrix}, \text{ e.g., see Figure 2b, where } \gamma = \tan \psi.$$

Note that the determinant in both cases is 1, i.e., there is no change in area (or volume in 3D). Note also that the matrix for pure shear is symmetric and therefore there is no rotational component to the strain, which is not the case for simple shear. In pure shear, the two lines parallel to the axes in Figure 2a do not rotate and therefore remain perpendicular to each other. In simple shear, the only line that does not rotate in Figure

2b is that which is parallel to the shear direction; this line also does not change its length during progressive shearing.

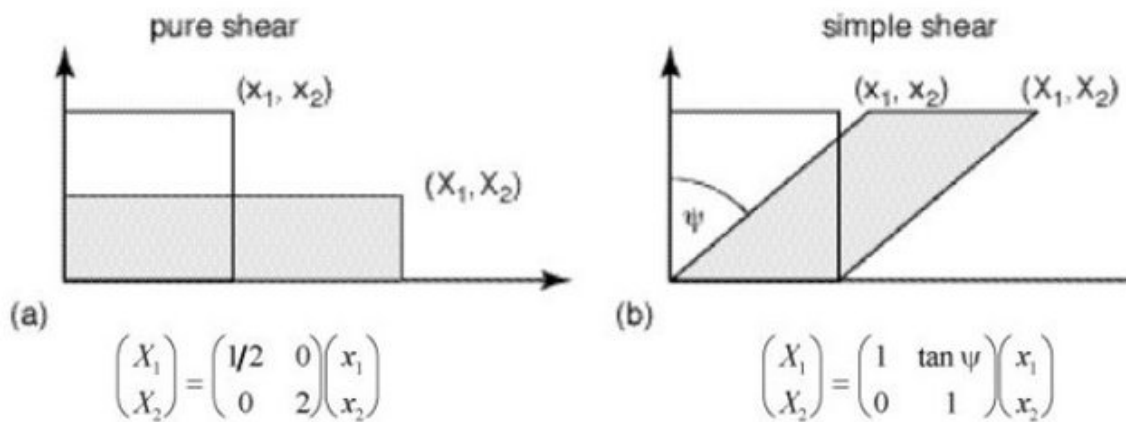


Figure 2. Geometry of (a) pure shear and (b) simple shear, where shear strain $\gamma = \tan \psi$.

Finite strain as described by such transformations considers only the final position relative to original position and can be visualized as a vector field joining original and final positions. As such, it ignores the actual progressive deformation path that consists of an infinite number of infinitesimal strain steps, which may vary with time and space. Strain clearly reflects spatial gradients in displacement and indeed this is how the infinitesimal strain is defined, namely $(e_{ij})_{inf} = (\partial u_i / \partial x_j + \partial u_j / \partial x_i) / 2$.

Natural structures may be more related to finite strain (e.g., the shape of a deformed fossil) or to progressive strain (e.g., curved fiber growth tracking strain increments). For finite strain, the transformation can be viewed in two ways: the Eulerian description relative to initial position (as considered above) and the Lagrangian description relative to current position. In practical applications to structural geology, it is often the Lagrangian description that is more useful, since we observe the final deformed configuration and wish to estimate the deformation necessary to return it to the original form. The two descriptions are related via the inverse of the matrix \mathbf{A} , namely if $\mathbf{X} = \mathbf{A}\mathbf{x}$ then $\mathbf{x} = \mathbf{A}^{-1}\mathbf{X}$. For finite strain, the order of \mathbf{D} and \mathbf{R} above is important; this is not the case for infinitesimal strain. It should also be clear that stress as an instantaneous quantity can only be directly related to the corresponding infinitesimal strain and has no direct relationship to the finite strain accumulated over a period of time.

If the components of \mathbf{A} are themselves constants independent of position, then the strain is homogeneous. Homogeneous strain implies that straight lines remain straight and parallel lines remain parallel (though the distance between the lines will change). Strain is in reality generally heterogeneous with, for example, straight lines becoming increasingly curved to develop the folds observed in the field (see Section 3.1). The scale of observation then becomes important: above a certain scale, deformation is markedly heterogeneous and, in polycrystalline and generally polymineralic rocks, deformation on a grain scale is also heterogeneous. However, on a sample or outcrop scale, the strain may be approximately homogeneous. This is obviously a primary consideration if a value of finite strain is to be estimated for a natural sample.

As noted in Section 2.1, a symmetric second order tensor such as **D** can always be transformed into a diagonal form for a specific set of orthogonal axes (called the principal axes). These axes are parallel to the only set of orthogonal lines that have remained orthogonal during deformation (i.e., there is no change in angle or “shear strain” between these lines) and two of the axes are parallel to directions of maximum and minimum relative change in length of lines (or “stretch”). The strain can be visualized as an ellipsoid, with major, minor and intermediate axes parallel to the principal axes. For an isotropic material (i.e., properties do not vary with direction), the principal axes of the stress ellipsoid will coincide with the principal axes of the resultant infinitesimal strain ellipsoid. For an anisotropic material, this is not the case. If the principal axes of finite and infinitesimal strain coincide, the deformation is coaxial and there is no rotational component. Otherwise, the rotational component is measured as the angle between the principal strain axes and the original orientation of the lines now parallel to the principal axes. However, even for coaxial deformation, the shape of the finite and infinitesimal ellipsoids is different (except for the trivial case of the very first infinitesimal strain increment). The fields in the respective ellipsoids for which lines are stretched or shortened, separated by surfaces of no length change, are therefore not coincident and lines can at any instant be:

- (1) stretched and continue stretching,
- (2) stretched but currently shortening,
- (3) shortened and continue shortening,
- (4) shortened but currently stretching.

Added to this are the special cases where the length is currently the same as the original (no finite longitudinal strain) or currently not changing length (no infinitesimal stretch). It is the combination of these fields that directly explains the observed natural deformation structures, since any surface can be considered in terms of a series of lines.

-
-
-

TO ACCESS ALL THE 29 PAGES OF THIS CHAPTER,
Visit: <http://www.eolss.net/Eolss-sampleAllChapter.aspx>

Bibliography

Abbassi, M. and Mancktelow, N.S. (1990). The effect of initial perturbation shape and symmetry on fold development. *Journal of Structural Geology* **12**, 273-282. [Analog modeling study of the influence of initial irregularities on final fold shape].

Amadei, B. and Stephansson, O. (1997). *Rock stress and its measurement*, 490 pp. London: Chapman & Hall. [An extensive review of fundamentals and practical methods for measuring current rock stress].

Barenblatt, G.I. (1996). *Scaling, self-similarity, and intermediate asymptotics*, 386 pp. Cambridge: Cambridge University Press [The most recent expanded edition of the classic text on scaling and dimensional analysis].

Bell, R.T. and Currie, J.B. (1964). Photoelastic experiments related to structural geology. *Proceedings of the Geological Association of Canada* **15**, 33-51. [Study of contours in stress magnitude using the photoelastic method].

Biot, M.A. (1957). Folding instability of a layered viscoelastic medium under compression. *Proceedings of the Royal Society, London A* **242**, 444-454. [Classic paper on buckle folding].

Biot, M.A. (1961). Theory of folding of stratified visco-elastic media and its implications in tectonics and orogenesis. *Geological Society of America Bulletin* **72**, 1595-1620. [Overview paper of much of the author's groundbreaking work on buckle folding].

Brun, J.P. and Cobbold, P.R. (1980). Strain heating and thermal softening in continental shear zones: a review. *Journal of Structural Geology* **2**, 149-158. [Overview of the potential for shear heating and thermal runaway in shear zones].

Dieterich, J.H. and Carter, N.L. (1969). Stress history of folding. *American Journal of Science* **267**, 129-154. [Early example of numerical modeling applied to folding].

Fletcher, R.C. (1974). Wavelength selection in the folding of a single layer with power-law rheology. *American Journal of Science* **274**, 1029-1043. [Analytical derivation of the initial growth rate of sinusoidal single-layer folds without the restrictive assumptions of thin-plate theory].

Flinn, D. (1962). On folding during three dimensional progressive deformation. *Quarterly Journal of the Geological Society of London* **118**, 385-428. [Representation of 3D strain on a 2D plot, now known as the "Flinn diagram"].

Fry, N. (1979). Random point distributions and strain measurement in rocks. *Tectonophysics* **60**, 89-105. [Classic paper outlining the "Fry method" for finite strain determination using the center-to-center technique].

Grujic, D. (1993). The influence of initial fold geometry on Type 1 and Type 2 interference patterns: an experimental approach. *Journal of Structural Geology*, **15**: 293-307. [Analog modeling study of fold interference structures]

Hubbert, M.K. (1937). Theory of scale models as applied to the study of geologic structures. *Geological Society of America Bulletin* **48**, 1459-1520. [Excellent and thorough consideration of the scaling of physical models].

Jaeger, J.C. (1969). *Elasticity, fracture and flow with engineering and geological applications, third edition*, 268 pp. London: Chapman and Hall. [Compact summary of stress, strain, and rock mechanics].

Lisle, R.J. (1985). Geological strain analysis. *A Manual for the R/Φ Technique*, 99 pp. Oxford: Pergamon Press. [Practical manual for use of the R/Φ technique for practical strain determination].

Mancktelow, N.S. (1999). Finite-element modelling of single-layer folding in elasto-viscous materials: the effect of initial perturbation geometry. *Journal of Structural Geology* **21**, 161-177. [Numerical modeling applied to understanding the effect of initial perturbations on fold development].

Mase G.E. (1970). *Theory and Problems of Continuum Mechanics*. 221 pp. New York: Schaum's Outline Series, McGraw Hill Book Company. [Concise, but thorough, introduction into tensors and the mathematical description of stress, strain, elasticity, plasticity and flow in a continuum].

Means W.D., Hobbs, B.E., Lister, G.S. and Williams, P.F. (1980). Vorticity and non-coaxiality in progressive deformations. *Journal of Structural Geology* **2(3)**, 371-378. [Original introduction to structural geologists of the fundamental concepts related to flow in a clear and relevant way, based on large body of earlier work in continuum mechanics, e.g., see summary in Mase, 1970].

Odonne, F. and Vialon, P. (1987). Hinge migration as a mechanism of superimposed folding. *Journal of Structural Geology* **9**, 835-844. [Analog modeling study of fold interference].

Pennacchioni, G., Fasolo, L., Morandi Cecchi, M. and Salasnich, L. (2000). Finite-element modelling of simple shear flow in Newtonian and non-Newtonian fluids around a circular rigid particle. *Journal of Structural Geology* **22**, 683-692. [Numerical modeling of rotation of a rigid particle].

Peresson, H. and Decker, K. (1997). The Tertiary dynamics of the northern Eastern Alps (Austria): changing palaeostresses in a collisional plate boundary. *Tectonophysics* **272**, 125-157. [Good example of the practical application of stratigraphically controlled palaeostress analysis].

Price N.J. and Cosgrove J.W. (1990). *Analysis of Geological Structures*. 502 pp. Cambridge: Cambridge University Press. [Well-balanced mixture of description of natural deformation structures and mechanical analysis of their formation].

Quiblier, J.A., Tremolieres, P. and Zinszner, B. (1980). A tentative fault propagation description by three-dimensional finite-element analysis. *Tectonophysics* **68**, 199-212. [Numerical modeling of fault propagation].

Ramberg, H. (1961). Contact strain and fold instability of a multilayered body under compression. *Geologische Rundschau* **51**, 405-439. [Classic paper for buckle folding of multilayers].

Ramberg, H. (1981). *Gravity, Deformation and the Earth's Crust*. 452 pp. London: Academic Press. [Classic reference with good overview of analytical and physical modeling techniques and results at that time].

Ramsay, J.G. (1967). *Folding and Fracturing of Rocks*. 568 pp. New York: McGraw-Hill. [Still a classic reference for the geometry of strained rocks].

Ramsay, J.G. and Huber M.I. (1983). *The Techniques of Modern Structural Geology. Volume 1: Strain Analysis*, 307 pp. London: Academic Press. [The basic text on the geometry of deformation structures].

Ramsay, J.G. and Huber M.I. (1987). *The Techniques of Modern Structural Geology. Volume 2: Folds and Fractures*, 309-700. London: Academic Press. [The basic text on the geometry of deformation structures].

Ramsay, J.G. and Graham, R.H. (1970). Strain variation in shear belts. *Canadian Journal of Earth Sciences* **7**, 786-813. [The classic paper for the geometry of natural shear zones].

Ramsay, J.G. and Lisle, R.J. (2000). *The Techniques of Modern Structural Geology. Volume 3: Applications of continuum mechanics in structural geology*, 701-1061. London: Academic Press. [An introduction to analytical and numerical modelling methods].

Ranalli, G. (1995). *Rheology of the Earth (Second Edition)*, 413 pp. London: Chapman & Hall. [Thoroughly developed, more “geophysical” approach to rock deformation].

Schreurs, G. and Colletta, B. (1998). Analogue modelling of faulting in zones of continental transpression and transtension, In: Holdsworth, R.E., Strachan, R.A. and Dewey, J.F. (editors), Continental transpression and transtensional tectonics. *Geological Society of London Special Publication* **135**, 59-79. [Example of use of computer tomography of analog models to study progressive fault development].

Smith, R.B. (1975). Unified theory of the onset of folding, boudinage and mullion structure. *Geological Society of America Bulletin* **86**, 1601-1609. [Analytical models of buckle fold development].

Strömgård, K.-E. (1973). Stress distribution during formation of boudinage and pressure shadows. *Tectonophysics* **16**, 215-248. [Analytical models of stress distribution during boudin formation].

Weijermars, R. and Schmeling, H. (1986). Scaling of Newtonian and non-Newtonian fluid dynamics without inertia for quantitative modelling of rock flow due to gravity (including the concept of

rheological similarity). *Physics of the Earth and Planetary Interiors* **43**, 316-330. [Analysis of the need for rheological similarity in analog models].

Biographical Sketch

Neil Mancktelow is a senior lecturer in the geology department at the ETH in Zürich, Switzerland. He has an international reputation in a variety of research fields related to structural geology in the widest sense. These include Alpine tectonics as well as numerical and analogue modeling of outcrop scale structures. He has always had a particular interest in the conceptual explanation of geological problems.